Involvement of Artemis in nonhomologous end-joining during immunoglobulin class switch recombination

Likun Du,[1] Mirjam van der Burg,[2] Sergey W. Popov,[1] Ashwin Kotnis,[1] Jacques J.M. van Dongen,[2] Andrew R. Gennery,[3] and Qiang Pan-Hammarström[1]

[1]Clinical Immunology, Department of Laboratory Medicine, Karolinska Institutet at Karolinska University Hospital Huddinge, SE-14186, Stockholm, Sweden
[2]Department of Immunology, Erasmus Medical Center, 3000 CA, Rotterdam, Netherlands
[3]Department of Pediatric Immunology, Newcastle General Hospital, Newcastle NE4 6BE, England, UK

DNA double-strand breaks (DSBs) introduced in the switch (S) regions are intermediates during immunoglobulin class switch recombination (CSR). These breaks are subsequently recognized, processed, and joined, leading to recombination of the two S regions. Nonhomologous end-joining (NHEJ) is believed to be the principle mechanism involved in DSB repair during CSR. One important component in NHEJ, Artemis, has however been considered to be dispensable for efficient CSR. In this study, we have characterized the S recombinational junctions from Artemis-deficient human B cells. Sμ–Sα junctions could be amplified from all patients tested and were characterized by a complete lack of "direct" end-joining and a remarkable shift in the use of an alternative, microhomology-based end-joining pathway. Sμ–Sγ junctions could only be amplified from one patient who carries "hypomorphic" mutations. Although these Sμ–Sγ junctions appear to be normal, a significant increase of an unusual type of sequential switching from immunoglobulin (Ig)M, through one IgG subclass, to a different IgG subclass was observed, and the Sγ–Sγ junctions showed long microhomologies. Thus, when the function of Artemis is impaired, varying modes of CSR junction resolution may be used for different S regions. Our findings strongly link Artemis to the predominant NHEJ pathway during CSR.

CORRESPONDENCE
Qiang Pan-Hammarström:
Qiang.Pan-Hammarstrom@ki.se

Abbreviations used: CID, combined immunodeficiency; CSR, class switch recombination; DSB, double-strand break; HR, homologous recombination; NHEJ, nonhomologous end-joining; S, switch; SCID, severe CID; SHM, somatic hypermutation.

DNA double-strand breaks (DSBs) represent serious threats to cell survival, and inappropriate response to this threat may lead to genome instability and development of cancer. DSBs can be caused by exogenous agents such as ionizing radiation or certain chemicals, but can also arise during normal endogenous processes, including DNA replication and meiosis. There are two major pathways for repair of DSBs: homologous recombination (HR) and nonhomologous end-joining (NHEJ). The former is dependent on sequence homology, is error free, and is most active in the late S/G2 phase of the cell cycle. The latter utilizes little, or no, sequence homology, is often imprecise, functions throughout the cell cycle, and is considered to be the principle mechanism used in vertebrate cells (1, 2). The classical NHEJ machinery requires a set of proteins, including Ku70, Ku80, DNA-PKcs, DNA ligase IV, XRCC4, Artemis and the recently identified XLF (Cernunnos) (3, 4). Alternative, or backup, NHEJ pathway(s), usually involving terminal microhomologies, have also been described (1, 2).

DSBs are also intermediates for V(D)J recombination and class switch recombination (CSR), two physiological processes that are important for the generation of functional antigen receptors. During early B and T lymphocyte development, V(D)J recombination takes place to assemble the variable (V) region of the T cell receptor and Ig genes, giving rise to a large repertoire of specificities (5). In mature B cells, CSR allows previously rearranged Ig heavy-chain V domains to be expressed in association

The Rockefeller University Press $30.00
J. Exp. Med. Vol. 205 No. 13 3031-3040
www.jem.org/cgi/doi/10.1084/jem.20081915

with a different constant (C) region, leading to production of different isotypes (IgG, IgA, or IgE) with improved biological effector functions (6, 7). The seven known components of the classical NHEJ are all essential for the V(D)J recombination process (4, 5) and the "alternative NHEJ" pathway seems to be suppressed by the Rag proteins and operative (still inefficiently) only when the classical NHEJ fails (8, 9). In contrast to V(D)J recombination, the alternative, microhomology-based end-joining pathway is functional to some extent during CSR in normal cells, and is more effective when the classical NHEJ fails (10–12).

Five components of the classical NHEJ (Ku70, Ku80, DNA-PKcs, DNA ligase IV, and XRCC4) have been shown to be important for CSR (11–16). XLF deficiency has been described in a few patients with growth retardation, microcephaly, and immunodeficiency (4). The serum levels of IgA and IgG in these patients are low or absent, accompanied by normal or high levels of IgM, suggesting an involvement of XLF in CSR (4). In support of this notion, a recent study has shown that XLF-deficient mouse B cells are moderately defective in CSR (17). Artemis has only been considered to have a restricted role in V(D)J recombination (hairpin opening activity) and to be altogether dispensable for CSR (18).

In humans, mutations in *Artemis* (*DCLRE1c*) result in $T^-B^-NK^+$ severe combined immunodeficiency (SCID) associated with increased radiosensitivity, a disorder that is characterized by a severe defect in V(D)J recombination leading to an early arrest of both B and T cell maturation (19). Hypomorphic mutations in the gene have also been described and are associated either with Omenn's syndrome, which is a "leaky" form of $T^-B^-NK^+$ SCID (20), or CID (21, 22). The latter group of patients (with CID) does have polyclonal T and B lymphocyte populations, albeit in reduced numbers, but with extremely low levels, or absence of serum IgG and IgA (21, 22). It is possible that a lower efficiency of CSR, in addition to the defective V(D)J recombination, contributes to the immunodeficiency observed in these patients. Furthermore, Artemis is absolutely required for repairing ~10% of the DSBs induced by γ irradiation, representing breaks rejoined with a slow kinetics in mammalian cells (23). It is tempting to speculate that Artemis may also have a role in CSR, i.e., in the processing of a subset of DSBs with more complex ends where the repair requires a longer time. In support of this hypothesis, Franco et al. have recently shown that Artemis-deficient B cells, activated to undergo CSR, showed an increased number of chromosomal breaks at the Ig locus (24). To further investigate the role of Artemis in end-joining during CSR, we therefore performed a detailed analysis of the switch (S) recombination junctions in B cells from Artemis-deficient patients.

RESULTS

Switching to IgA in Artemis-deficient patients

Genomic DNA was prepared from peripheral blood from 4 Artemis-deficient patients (Table I) and 14 age-matched controls. Patients A1, A7, and A8 were diagnosed with $T^-B^-NK^+$ SCID, and patient AKE was diagnosed with progressive CID. A1 and A7 carry homozygous gross deletions in the *Artemis* gene, whereas A8 has a homozygous deletion of five nucleotides resulting in a frame shift and premature stop codon (Table I). AKE is a compound heterozygote with a 3-bp deletion on one allele and a missense mutation on the other allele, resulting in Artemis proteins with an L70 deletion or a G126D substitution (22, 25). Both mutations have an impact on Artemis function, and the level of Artemis protein is greatly reduced in the patient's cells (22). The mutations from this patient were, however, less devastating, or "hypomorphic," as both the clinical and cellular phenotypes were less severe compared with the other three patients.

To determine whether CSR was affected by a lack of functional Artemis, individual Sμ–Sα junctions were amplified using our previously developed nested-PCR assay (26). The number of Sμ–Sα fragments was determined from 10 PCR reactions run in parallel using DNA from each individual. As shown in Fig. 1 A, the number and intensity of amplified bands were lower in the Artemis patients. Patient AKE had a normal number of B cells but the number of clones that had switched to IgA was 3–9 fold reduced, as estimated by serial titration of control DNA templates. Patients A1, A7, and A8 had extremely low numbers of B cells (undetectable by routine FACS analysis), thus it is difficult to estimate the proportion of B cells that have switched to IgA. It is important to note that Sμ–Sα fragments could still be amplified from DNA samples from all three patients, including patients A1 and A7, who carry large genomic deletions and with no functional protein (Fig. 1 A and not depicted). The weak bands amplified from the patients, indeed, represent bona fide CSR junctions (see the following paragraph). Residual IgA switching thus appears to occur even in the complete absence of functional Artemis protein.

Altered pattern of Sμ–Sα recombination junctions

The amplified Sμ–Sα fragments were subsequently sequenced and compared with germline Sμ and Sα sequences to define the switch junctions. Altogether, 54 unique Sμ–Sα sequences from Artemis-deficient patients were obtained (Fig. S1, available at http://www.jem.org/cgi/content/full/jem.20081915/DC1) and compared with 141 Sμ–Sα fragments from age-matched controls (Fig. S2). One sequence from each patient and 4 junctions from controls are shown in Fig. 1 B.

Switching to α1 occurred more often than to α2 both in patients and controls (65 and 77%, respectively). Sequential switching through Sγ, involving two nonhomologous recombination processes (Sμ to Sγ and Sγ to Sα), was not observed in the patients, although it represents ~3% (4 out of 141) of IgA switching events in the age-matched controls (7% in our previously described adult controls [11, 26]).

There was a strikingly high degree of overlap between the Sμ and Sα sequences in recombination junctions derived from the Artemis patients (8.0 ± 6.2 vs. 3.9 ± 5.1 nucleotides in controls; Fig. 1, B and C, and Table II; Student's t test, $P < 0.0001$). This was caused by a significantly decreased proportion of

Table I. Serum immunoglobulin levels in Artemis patients

Patient ID	Diagnosis	Age at sampling	B cell count	Serum Ig levels (g/liter)			*Artemis* mutations	References
			%	IgM	IgG	IgA		
A1	$T^-B^-NK^+$ SCID	5 mo	<0.01	NA[a]	NA	NA	deletion of exon 10, 11, 12 (ho)	(42)
A7	$T^-B^-NK^+$ SCID	7 mo	0	<0.04	3.38[b]	<0.07	deletion of exon 1, 2, 3 (ho)	(43)
A8	$T^-B^-NK^+$ SCID	6 mo	<0.01	0.13	5.7[b]	0.1	1391-1395delGAATC (ho)	(39)
AKE	CID	4 yr	33[c]	2.3	<2.0	<0.4	207-209delGTT (he)/377G>A (he)	(22, 25)

[a]NA, not available.
[b]IgG could be of maternal origin.
[c]The absolute B cell count: 353 cells/μl.

Sμ–Sα junctions with no microhomology (11 vs. 42% in controls; χ^2 test, $P < 0.001$) and a significantly increased proportion of junctions exhibiting a long microhomology of ≥10 bp (39 vs. 16%; χ^2 test, $P < 0.0001$; Fig. 1 C and Table II). When one mismatch was allowed at either side of the recombination breakpoint, a majority of the junctions were flanked by ≥10/11 bp of imperfect repeats (43 + 41 = 84 vs. 33% in controls; χ^2 test, $P < 0.001$; Table S1, available at http://www.jem.org/cgi/content/full/jem.20081915/DC1). This dramatic shift in the use of long microhomologies or imperfect repeats in the Sμ–Sα junctions has previously only been observed in patients with DNA ligase IV deficiency (Table II and Table S1) (11), and, to a lesser degree, in patients with a subtype of the Hyper IgM syndrome (27) and ataxia-telangiectasia (A-T, ATM deficient) (26).

The six Sμ–Sα junctions (11% of total junctions) from Artemis-deficient patients that did not exhibit a perfect sequence homology (0 bp microhomology) can all be defined as having a 1-bp insertion (Table II). Typically, these junctions were also flanked by long imperfect repeats (A7-1 in Fig. 1 B). In controls, ∼60% of the Sμ–Sα junctions with 0-bp microhomology could be classified as having a 1-bp insertion (25% of total junctions), and these junctions were not necessarily associated with long imperfect repeats (C29-271 in Fig. 1 B). The remaining 40% of control junctions with 0 bp microhomology could be defined as "direct" end-joining, i.e., no microhomology and no insertions (exemplified by C5-230 and C29-261 in Fig. 1 B; 18% of total junctions, Table II). When a stricter rule was applied, i.e., no microhomology, no insertions, and no mutations close to the junctions, there were still 10% of the total control junctions (14 out of 137, exemplified by C5-230) that could be classified as "perfect" or "precise direct" end-joining. Thus, in the absence of Artemis, recombination of the Sμ and Sα regions is heavily dependent on the alternative end-joining pathway(s) that require long microhomologies, and the ability of cells to join these two S regions by direct end-joining mechanism(s) appears to be totally lost.

The frequency of mutations around the Sμ–Sα junctions (± 15 bp) was significantly reduced in Artemis-deficient patients (5.6 vs. 12.4 mutations/1,000 bp; χ^2 test, $P < 0.05$; Table III). Furthermore, the general pattern of base substitutions was significantly altered as a majority of the mutations occurred at A/T residues (89 vs. 25% in controls; χ^2 test, $P < 0.001$; Table III). Similarly, most of the 1-bp insertions also occurred at A/T sites (80 vs. 15% in controls; χ^2 test, $P < 0.001$). The reduced rate of mutations or insertions close to, or at, the CSR junctions could be a feature coupled to the increased requirement for a long microhomology, as in ATM- or DNA ligase IV–deficient patients (11, 26). The dominant A/T mutations/insertions around, or at, the Sμ–Sα junctions, is, however, a unique feature in Artemis-deficient patients, as the few mutations observed in ATM- or DNA ligase IV–deficient patients were mainly located at G/C sites (83% for both patient groups; Table III).

Point mutations can often be observed in the recombined Sμ region, away from (starting 15 bp upstream) the recombination breakpoints (28). The pattern of these mutations is similar to those in the V regions (thus they are referred to as somatic hypermutation [SHM]-like), but different from those close to, or at, the recombination breakpoints (±15 bp) (28). In Artemis-deficient patients, SHM-like mutations were observed at a slightly lower (but not significantly different) level as compared with those from controls (Table III). However, the general pattern of base substitutions was again altered, occurring more frequently at A/T sites (58 vs. 30% in controls; χ^2 test, $P < 0.001$) and less often being associated with the SHM hotspot motifs (RGYW/WRCY; R, A or G; Y, C or T; W, A or T; Table III).

As patients A1, A7, and A8 had barely detectable peripheral B cells, it is possible that the Sμ–Sα junctions amplified for these patients originate from a very minor and potentially skewed B cell pool. However, as a vast majority of the Sμ–Sα junctions amplified from patients A1, A7, and A8 (28 of 29 junctions) had a unique sequence, the B cell pool in these patients is still considerable. Furthermore, the pattern of Sμ–Sα junctions in these three patients is very similar to patient AKE, who had a normal number of B cells. Long microhomologies and a complete lack of direct end-joining are characteristic for all patients. The frequency and pattern of mutations at the Sμ–Sα junctions, or in the recombined Sμ regions, is also very similar (unpublished data). Thus, the altered Sμ–Sα junctions in patients A1, A7, and A8 is unlikely to be caused by a restricted B cell pool.

Our previously described 154 control Sμ–Sα junctions were amplified from PBL from 17 healthy adults (11, 26), whereas the 137 control Sμ–Sα junctions described here were obtained from 14 healthy children (1–6 yr old). It is

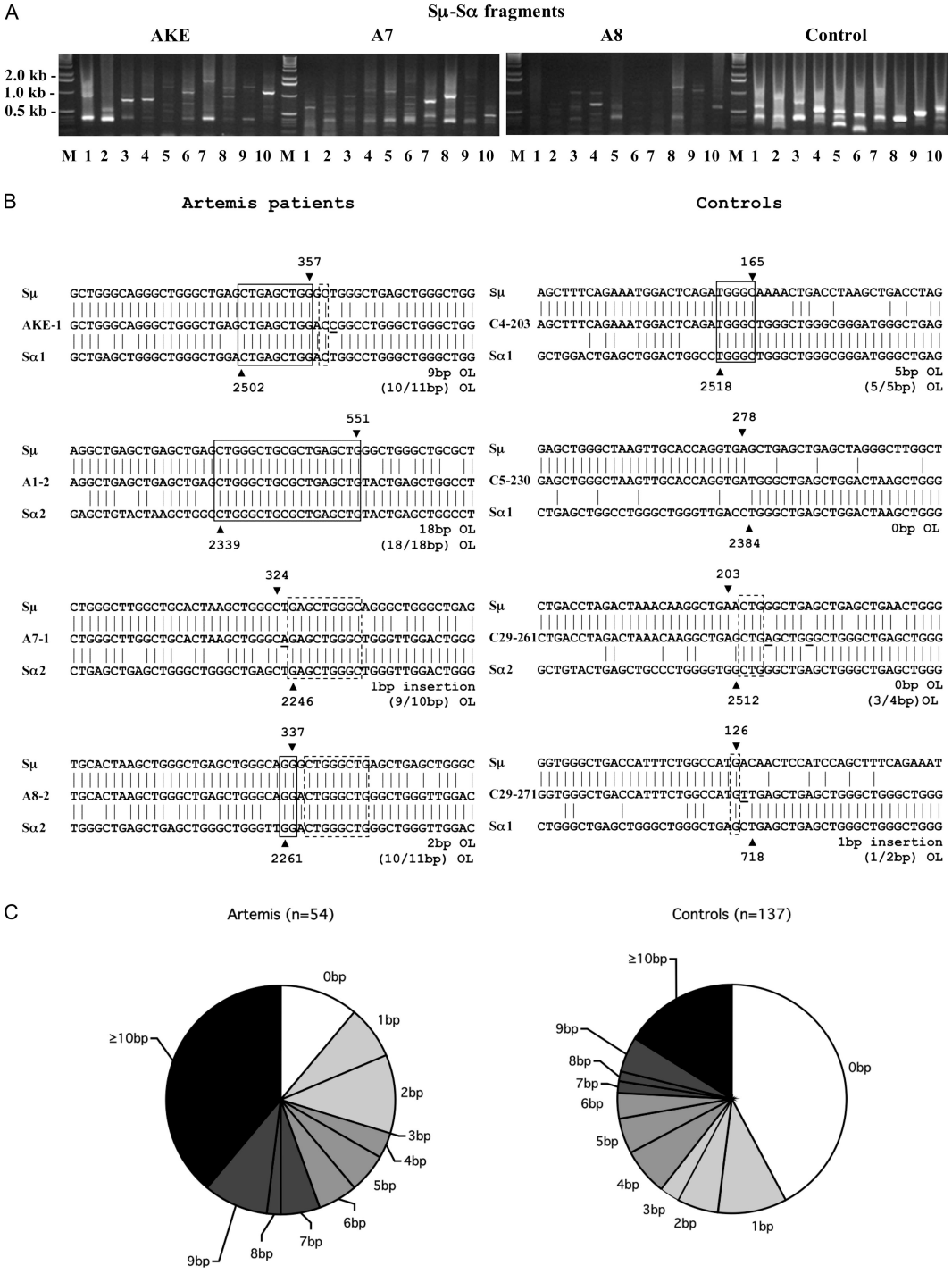

Figure 1. Characterization of Sμ–Sα junctions in Artemis-deficient patients. (A) PCR amplification of Sμ–Sα fragments. Three experiments were performed and a representative example is shown in the figure. The number of Sμ–Sα fragments was determined from 10 PCR reactions run in parallel (lane 1–10) using DNA from each individual. M, molecular weight marker (1-kb DNA ladder from Invitrogen). (B) Sequence of Sμ–Sα junctions. The Sμ and Sα sequences are aligned above and below the recombination junctional sequences. Microhomology is indicated by a box (solid line). Imperfect repeat was determined by identifying the longest overlap region at the switch junction by allowing one mismatch on either side of the breakpoints (the extra nucleotide identified beyond the perfectly matched sequence identity is boxed by a dotted line). OL, overlap. The Sμ and Sα breakpoints for each switch fragment are indicated by ▼ and ▲, respectively, and their positions in the germ line sequences are indicated on top of or below the arrowheads. (C) Pie charts demonstrate the microhomology usage at Sμ–Sα junctions in patients and controls. The proportion of switch junctions with a given size of perfectly matched short homology is indicated by the size of the slices.

Table II. Characterization of Sμ–Sα and Sμ–Sγ junctions[a,b]

	Perfectly matched short homology						Total no. of S fragments
	0 bp		1–3 bp	4–6 bp	7–9 bp	≥10 bp	
	1-bp insertions	No insertions					
Sμ–Sα							
Artemis$^{-/-}$	**6 (11%)***	**0 (0%)****	10 (19%)	8 (15%)	9 (17%)	**21 (39%)*****	54
Controls (1-6 y)	34 (25%)	24 (18%)	25 (18%)	21 (15%)	11 (8%)	22 (16%)	137
Ligase IV$^{-/-}$	**1 (3%)****	**0 (0%)*****	7 (23%)	4 (13%)	4 (13%)	**14 (47%)*****	30
ATM$^{-/-}$	**1 (2%)*****	**1 (2%)****	15 (34%)	9 (20%)	5 (11%)	**13 (30%)*****	44
Controls (adults)	39 (25%)	28 (18%)	56 (36%)	15 (10%)	11 (7%)	5 (3%)	154
Sμ–Sγ							
Artemis$^{-/-}$[c]	4 (17%)	5 (21%)	14 (58%)	1 (4%)	0 (0%)	0 (0%)	24
Controls (1-6 y)	9 (16%)	13 (22%)	26 (45%)	10 (17%)	0 (0%)	0 (0%)	58
Ligase IV$^{-/-}$	**11 (32%)***	4 (12%)	15 (44%)	4 (12%)	0 (0%)	0 (0%)	34
ATM$^{-/-}$	3 (8%)	3 (8%)	23 (61%)	**7 (18%)***	2 (5%)	0 (0%)	38
Controls (adults)	7 (12%)	12 (20%)	37 (63%)	3 (5%)	0 (0%)	0 (0%)	59

[a]The switch junctions from Artemis-deficient patients were compared with those from age matched controls (1-6 yr of age), whereas the switch junctions from DNA ligase IV– or ATM-deficient patients were compared with adult controls. Statistical analysis was performed using χ^2 test. Statistically significant differences are shown in bold. * $P < 0.05$; ** $P < 0.01$; *** $P < 0.001$.

[b]The data from DNA ligase IV– and ATM-deficient patients and the adult controls have previously been partially described (11, 26, 30).

[c]The Sμ–Sγ junctions were obtained from patient AKE.

worth noting that there are some differences between the two groups. Thus, the proportion of Sμ–Sα junctions with a short microhomology (1–3 bp) was significantly decreased in the younger controls (18 vs. 36% in adult controls; χ^2 test, $P < 0.001$; Table II), whereas the proportion of junctions showing a long microhomology (≥10 bp) was significantly increased (16 vs. 3% in the adult controls; χ^2 test, $P < 0.001$; Table II). The proportion of junctions with 4–6 or 7–9 bp of microhomology is, however, similar in the two groups (Table II). Furthermore, the proportion of junctions with a 1-bp

Table III. Mutations in recombined Sμ–Sα fragments[a]

	No. of mutations					
	AT versus GC mutations %	Transitions %	In RGYW/ WRCY motifs %	Total no. of mutations	No. of bp sequenced	Frequency (per 1,000 bp)
Close to the junction (±15 bp)						
Artemis$^{-/-}$	**8 versus 1 (89 vs. 11%)*****	5 (56%)	5 (56%)	9	1,620	**5.6***
Controls (1-6 y)	13 versus 38 (25 vs. 75%)	27 (53%)	28 (55%)	51	4,110	12.4
Ligase IV$^{-/-}$	1 versus 5 (17 vs. 83%)	2 (33%)	5 (83%)	6	900	6.7
ATM$^{-/-}$	1 versus 5 (17 vs. 83%)	1 (17%)	4 (67%)	6	1,320	**4.5****
Controls (adults)	11 versus 56 (16 vs. 84%)	30 (45%)	53 (79%)	67	4,590	14.6
Within Sμ (>15 bp upstream of the junction)						
Artemis$^{-/-}$	**38 versus 28 (58 vs. 42%)*****	43 (65%)	**37 (56%)***	66	15,508	4.3
Controls (1-6 yr)	42 versus 59 (30 vs. 70%)	95 (67%)	101 (72%)	141	26,569	5.3
Ligase IV$^{-/-}$	10 versus 8 (56 vs. 44%)	14 (78%)	13 (72%)	18	9,749	**1.8*****
ATM$^{-/-}$	**20 versus 16 (56 vs. 44%)***	**31 (86%)****	24 (67%)	36	1,1993	**3.0****
Controls (adults)	62 versus 105 (37 vs. 63%)	99 (59%)	117 (70%)	167	31,502	5.3

[a]Statistical analysis was performed using χ^2 test. Statistically significant differences are shown in bold. * $P < 0.05$; ** $P < 0.01$; *** $P < 0.001$.

insertion (25 vs. 25%), which is caused by direct end-joining (18 vs. 18%) or precise direct end-joining (10 vs. 10%), was identical between the two sets of controls. Moreover, the frequency and pattern of mutations around the junctions and upstream of the junctions in the young controls are similar to those previously described (Table III). Thus, most of the features of Sμ–Sα junctions are conserved among controls, regardless of age. There might, however, be some age-related variations in the use of microhomology-dependent end-joining pathways, and appropriate age-matched controls should therefore be included when studying the pattern of CSR junctions.

Switching to IgG in Artemis-deficient patients

Sμ–Sγ junctions were subsequently amplified using a nested-PCR assay (11, 29). Sμ–Sγ1, Sμ–Sγ2, and Sμ–Sγ3 fragments could be detected in cells from patient AKE using the respective Sγ-specific primers (Fig. 2 A). No Sμ–Sγ fragments could however, be amplified from patients A1, A7, and A8 (Fig. 2 A and not depicted). The weak bands observed in all lanes in patients A7 and A8 represent nonspecific amplification (Fig. 2 A). Switching to IgG could thus only be detected in cells from patient AKE, who carries hypomorphic mutations in *Artemis*.

Increased frequency of Sγ–Sγ sequential switching in patient AKE

The Sμ–Sγ fragments from patient AKE and age-matched controls were subsequently cloned and sequenced. Altogether, 24 unique Sμ–Sγ fragments from the patient were characterized (Fig. S3, available at http://www.jem.org/cgi/content/full/jem.20081915/DC1) and compared with 58 Sμ–Sγ fragments from age matched controls (Fig. S4). Most of the Sμ–Sγ fragments from the Artemis-deficient patient resulted from direct switching from IgM to various IgG subclasses. However, a substantial proportion of the fragments (5 out of 24, or 21%) showed clear evidence of sequential switching from IgM, through one IgG subclass (IgG3 or IgG1) to a different IgG subclass (IgG1 or IgG2, exemplified by AKE-1-3 and AKE-2-9 in Fig. 2 B). This is particularly true for switching to IgG2, where, in four out of five Sμ–Sγ2 fragments, sequential switching through Sγ1 or Sγ3 was evident. This type of sequential switching (Sμ–$S\gamma_x$–$S\gamma_y$) represents an extremely rare event in controls (1 out of 58, or 2% in the current controls; χ^2 test, $P < 0.01$; 0 of 59, or 0% in the previously described controls [30]; χ^2 test, $P < 0.001$).

At the Sμ–Sγ junctions, in contrast to the Sμ–Sα junctions, there was no significant difference in the length of microhomologies between the patient and control groups (1.4 ± 1.2 vs. 1.4 ± 1.6 bp in controls). Furthermore, the proportion of junctions with a 1-bp insertion (17 vs. 16%), caused by direct end joining (21 vs. 22%) or precise direct end-joining (8 vs. 7%), was almost identical between patient and controls (Table II and not depicted). Moreover, the frequency and pattern of mutations around the Sμ–Sγ junctions were similar between patient and controls (25 vs. 22 bp/1,000 bp, with G/C mutations being dominant). Thus, the general pattern of Sμ–Sγ junctions from this Artemis-deficient patient seems to be indistinguishable from controls.

It is worth noting, however, that in the Artemis-deficient patient, $S\gamma_x$–$S\gamma_y$ junctions resulting from recombination of two different Sγ regions, showed a strong preference for long microhomologies and imperfect repeats (Fig. 2 B and Fig. S5, available at http://www.jem.org/cgi/content/full/jem.20081915/DC1). All the junctions from the patient displayed microhomology, from 3 to 20 bp, with an average length of 12.0 ± 7.9 bp, whereas the only $S\gamma_x$–$S\gamma_y$ junction from controls had a 1-bp insertion. When one mismatch was allowed on either side of the junctions, the average length of imperfect repeats increased to 23.6 bp, which is even longer than that observed at the Sμ–Sα junctions from the patients (14.8 bp). Thus, when the function of Artemis is impaired, switching to IgG is more affected than switching to IgA, as the microhomology-based, alternative end-joining pathway cannot efficiently be used as a backup to recombine the Sμ and Sγ regions. This could be caused by the much lower degree of homology between Sμ and Sγ as compared with the Sμ and Sα regions, where the likelihood of obtaining a 7-, 10-, or 15-bp microhomology between Sμ–Sγ regions is 8-, 270-, and >1,000-fold lower, respectively, than in the Sμ–Sα regions (6). The different Sγ regions, however, share a very high degree of homology (6, 31), and once the Artemis-deficient cells have switched to IgG3 or IgG1, the alternative pathway can be used to drive a switch to a downstream IgG subclass, for instance IgG2, through a recombination of the two Sγ regions. In control cells, however, when the NHEJ functions normally, this pathway is almost never used.

DISCUSSION

Artemis was first identified as a nuclease that is specifically required for cleavage of hairpin intermediates generated during V(D)J recombination (19, 32). It has subsequently been shown to have a broader role in NHEJ, where it is required for repair of ∼10–20% of DSBs induced by γ irradiation or α particles (23). By analyzing the recombination junctions from Artemis-deficient patients, we now provide direct evidence that Artemis is also required for CSR, another gene rearrangement process that relies on NHEJ.

In Artemis-deficient patients, the Sμ–Sα junctions are characterized by a strong dependence of long microhomologies and a complete lack of direct end-joining, which constitutes ∼18% of the normal Sμ–Sα recombination events. These features are also noted in the Sμ–Sα junctions derived from DNA ligase IV– or ATM-deficient patients (Table II). This is different from the situation during V(D)J recombination, where the hairpin opening activity of Artemis is independent of ATM. It is, however, reminiscent of the situation after γ-irradiation, where Artemis, ATM, and DNA ligase IV function in a common repair pathway, responsible for processing of a subset of DSBs (23). Although the structure and chemistry of the DNA ends involved in this subset of DSBs are unknown, it has been proposed that these ends might be "damaged" or

more "complex" and thus require more time for repair and an involvement of the nuclease activity of Artemis (23).

Based on the known function of Artemis and the "morphology" of the Sμ–Sα junctions, we can deduce which types of DNA ends are involved in the direct end-joining process (Fig. 3). Both blunt and staggered ends have been detected in the S regions (33). Theoretically, like the recombination signal joint formation during V(D)J recombination, two blunt ends can be ligated directly, leading to a precise joining of the two S regions. However, as Artemis deficiency does not affect the efficiency and fidelity of the recombination signal joints (16), but impairs the direct end-joining during CSR, it is unlikely that such ligatable blunt ends exist in the CSR reaction without prior processing by Artemis. Artemis exhibits an intrinsic 5′- to 3′-exonuclease activity on single-stranded DNA and, when associated with and phosphorylated by DNA-PKcs, it shows endonuclease activity on overhangs and hairpins (32, 34–36). Cleavage of 5′

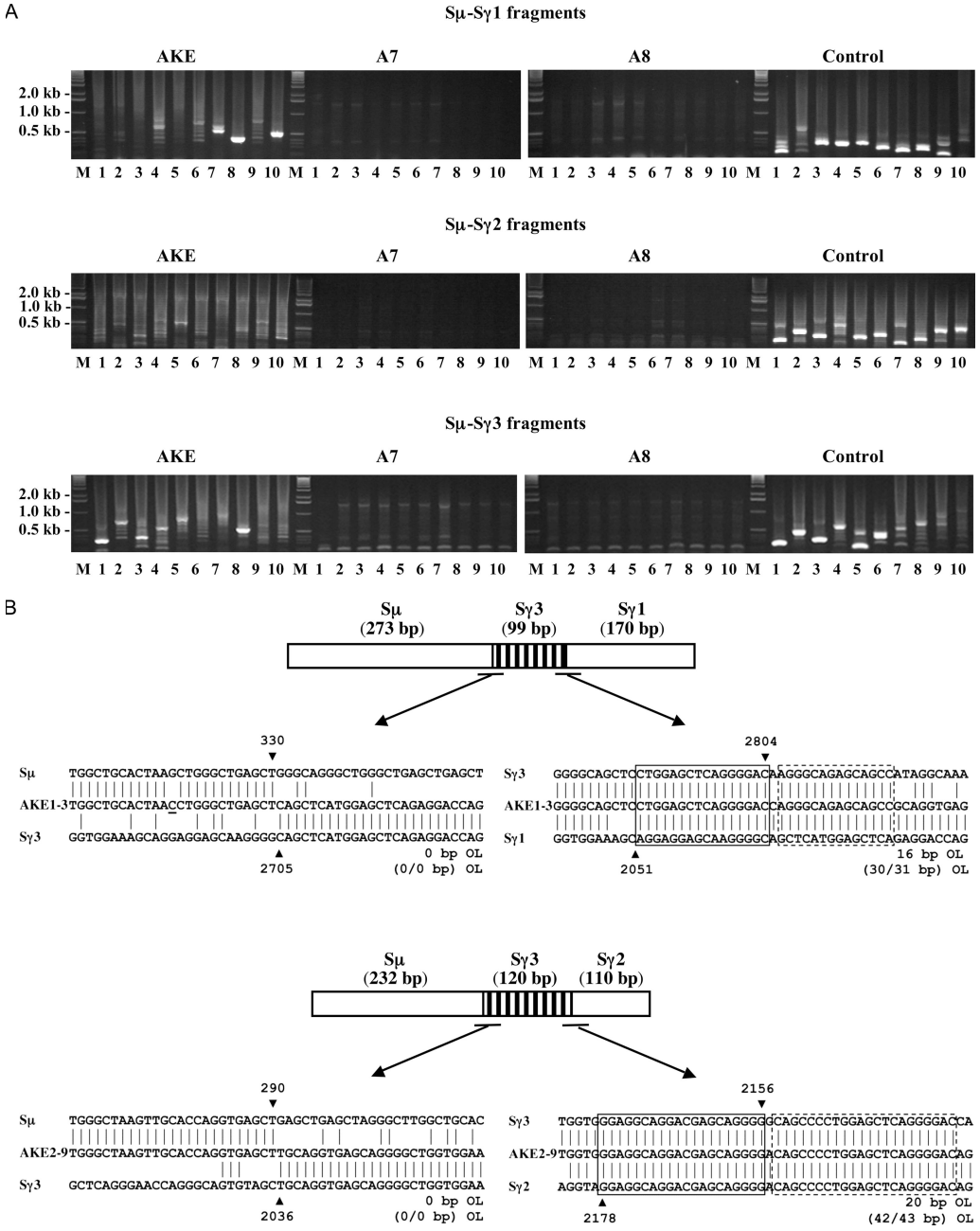

Figure 2. Characterization of Sμ–Sγ junctions in Artemis-deficient patients. (A) PCR amplification of Sμ–Sγ1, Sμ–Sγ2, and Sμ–Sγ3 fragments. Three experiments were performed and a representative example is shown in the figure. (B) Sμ–Sγ–Sγ sequential switching in AKE, showing the actual sequences of the Sμ–Sγ and Sγ–Sγ junctions.

overhangs by Artemis preferentially results in a blunt configuration, whereas cleavage of 3′ overhangs preferentially leaves short overhangs (35). It is possible that Artemis can process a pair of noncompatible ends to one blunt end and one 3′ overhang end, and Ku, DNA ligase IV/XRCC4, and XLF will subsequently promote ligation of such modified ends while retaining the 3′ overhang sequence (possibility 1 and 2 in Fig. 3) (37). No terminal microhomology is required in this type of end-joining, and this could explain the dependence of direct end-joining by Artemis, DNA ligase IV/XRCC4, and, possibly, XLF (unpublished data). It is also possible that processing by Artemis results in two blunt ends that can subsequently be directly ligated (possibility 3 in Fig. 3 B). Artemis may also convert terminally blocked blunt ends

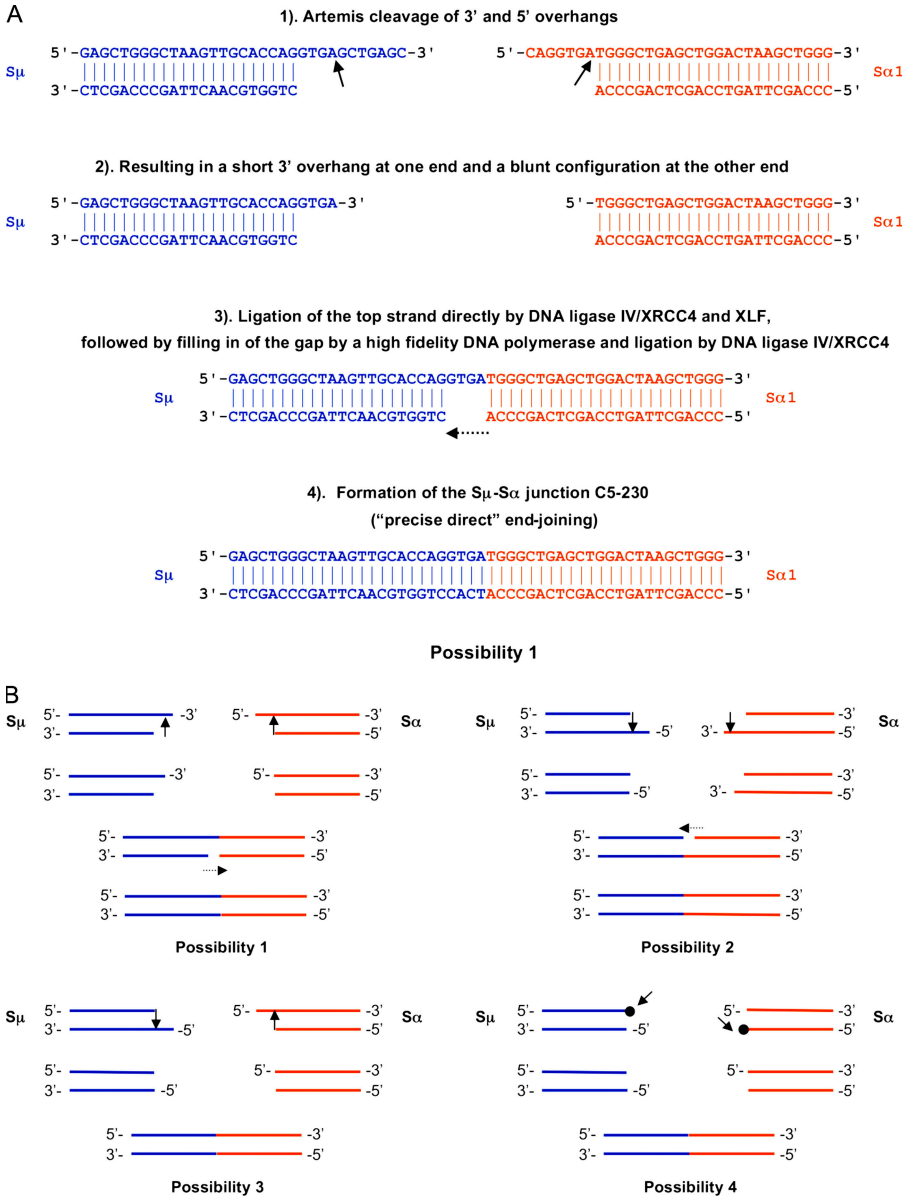

Figure 3. Hypothetical model for Artemis-dependent direct end-joining during CSR. The figure shows several possible ways of end processing by Artemis that may lead to the precise direct end-joining in junction C5-230 (a control junction presented in Fig. 1 B). (A) Possibility 1 is illustrated using the actual sequence of the junction. (B) Schematic models for possibilities 1–4. In possibility 1 and 2, Artemis cleavage of the 5′ overhang at one end, leads to a blunt configuration. On the other end, it cleaves the 3′ overhang, resulting in a short overhang with a few nucleotides. Solid arrows indicate the positions where Artemis acts. Ku, XRCC4/Ligase IV, and XLF promote the ligation of the 3′ overhanging hydroxyl group to the 5′ phosphate of the blunt end, leaving the other strand unjoined. The gap in the unjoined strand will then be filled in by a high fidelity DNA polymerase using the 3′ overhang sequence as a template (indicated by a dotted arrow). This strand will then be ligated by DNA ligase IV/XRCC4. In possiblity 3, both ends carry 5′ overhangs, and processing by Artemis results in the formation of two ligatable blunt ends. In possibility 4, Artemis converts the terminally blocked blunt ends (marked by filled circles) to ligatable blunt ends.

(such as those with 3′-phosphoglycolate or 3′-hydroxyl termini) with short overhangs and ligatable termini (possibility 4 in Fig. 3 B) (38). It is unclear, however, if such blocked blunt ends exist during the CSR reaction.

The key function of Artemis during V(D)J recombination is to open the hairpin structures at the coding ends. However, unlike the D_H–J_H junctions, where long stretches of palindromic nucleotides are present (39), the frequency and length of the potential palindromic sequences at the CSR junctions is not increased in the Artemis-deficient patients. Thus, the hairpin-opening activity of Artemis is unlikely to be required for CSR and a hairpin structure is probably not a major intermediate during CSR.

It is puzzling that patient AKE, who carries less devastating or "hypomorphic" mutations in *Artemis*, shows an altered pattern of Sμ–Sα junctions similar to the other three Artemis-deficient patients, but had a normal appearance of the Sμ–Sγ junctions. Lack of long microhomologies at the Sμ–Sγ junctions in this patient could be caused by the lack of sequence homology between Sμ and Sγ (6). The increased frequency of unusual Sμ–$Sγ_x$–$Sγ_y$ sequential switching in this patient and the long microhomologies observed in the $Sγ_x$–$Sγ_y$ junctions further suggest that when Artemis is defective, the alternative, microhomology-based end-joining machinery by itself is not a limiting factor for IgG switching. The normal proportion of direct joining at the Sμ–Sγ junctions in this patient is, however, more challenging to explain. It could be that the residual level of mutated Artemis protein in this patient can drive another type of alternative end-joining, with a slower kinetic. This hypothesis is supported by the results obtained from a cell line derived from this patient, where a subset of unrepaired DSBs observed at 2–3 d were ultimately repaired 4–6 d after irradiation (22). In contrast, this subset of DSBs remains unrepaired for a long time (up to 8 d) in Artemis-null cell lines. Thus, during IgA switching, the microhomology-based end-joining serves as an efficient alternative pathway in both Artemis-hypomorphic and null cells. IgG switching is, however, more affected in Artemis-null cells, as the microhomology-based pathway cannot operate efficiently during Sμ–Sγ recombination. Other alternative mechanism(s) may, however, be operating in Artemis- hypomorphic cells to join the Sμ–Sγ regions and the microhomology-based pathway can subsequently be used to recombine the Sγ–Sγ regions.

In summary, the altered pattern of CSR junctions in Artemis-deficient patients suggests that Artemis is required in the predominant NHEJ pathway during CSR. The functional role of Artemis in CSR probably relies on its endonuclease activity on 3′ or 5′ overhangs, rather than hairpin structures. Whether ATM or DNA-PKcs are required for this activity needs to be further investigated.

MATERIALS AND METHODS

Patients. The study included four Artemis-defective patients from four independent families. The clinical and genetic characterization has been described previously (see Table I and references therein). The mutations in the *Artemis* gene, B cell counts, and immunoglobulin levels of the patients are summarized in Table I. The institutional review board at the Karolinska Institutet approved the study.

Amplification and analysis of switch recombination junctions. Genomic DNA was purified from peripheral blood cells from patients and healthy blood donors. The amplification of Sμ–Sα and Sμ–Sγ fragments from in vivo switched cells was performed as previously described (11, 26, 29, 40, 41), except that a modified version of *Taq* polymerase (Go Taq; Promega) was used in the PCR reactions. With this modification, a two- to fourfold increase in sensitivity was achieved. The PCR-amplified switch fragments were gel purified (QIAGEN), cloned, and sequenced by an automated fluorescent sequencer in the MWG Company or in Macrogen.

The switch recombination breakpoints were determined by aligning the switch fragment sequences with the Sμ (X54713)/Sα1 (L19121)/Sα2 (AF030305) or Sμ/Sγ1 (U39737)/Sγ2 (U39934)/Sγ3 (U39935)/Sγ4 (Y12547-52) sequences. Analysis of microhomology/imperfect repeat usage and mutation pattern at the switch junctions was performed as previously described (26, 28).

Online supplemental material. The sequence of Sμ–Sα, Sμ–Sγ, and Sγ–Sγ junctions from Artemis patients and controls are presented in Figs. S1–S5. A summary of imperfect repeats at the Sμ–Sα junctions from Artemis patients and controls is presented in Table S1.Online supplemental material is available at http://www.jem.org/cgi/content/full/jem.20081915/DC1.

This work was supported by the Swedish Research Council, the Swedish Cancer Foundation, the Swedish Society for Medicine, and the "KID" program from the Karolinska Institutet.

The authors have no conflicting financial interests.

Submitted: 26 August 2008
Accepted: 6 November 2008

REFERENCES

1. Lieber, M.R. 2008. The mechanism of human nonhomologous DNA end joining. *J. Biol. Chem.* 283:1–5.
2. Lieber, M.R., Y. Ma, U. Pannicke, and K. Schwarz. 2003. Mechanism and regulation of human non-homologous DNA end-joining. *Nat. Rev. Mol. Cell Biol.* 4:712–720.
3. Ahnesorg, P., P. Smith, and S.P. Jackson. 2006. XLF interacts with the XRCC4-DNA ligase IV complex to promote DNA nonhomologous end-joining. *Cell.* 124:301–313.
4. Buck, D., L. Malivert, R. de Chasseval, A. Barraud, M.C. Fondaneche, O. Sanal, A. Plebani, J.L. Stephan, M. Hufnagel, F. le Deist, et al. 2006. Cernunnos, a novel nonhomologous end-joining factor, is mutated in human immunodeficiency with microcephaly. *Cell.* 124:287–299.
5. Jung, D., C. Giallourakis, R. Mostoslavsky, and F.W. Alt. 2006. Mechanism and control of V(D)J recombination at the immunoglobulin heavy chain locus. *Annu. Rev. Immunol.* 24:541–570.
6. Pan-Hammarstrom, Q., Y. Zhao, and L. Hammarstrom. 2007. Class switch recombination: a comparison between mouse and human. *Adv. Immunol.* 93:1–61.
7. Stavnezer, J., J.E. Guikema, and C.E. Schrader. 2008. Mechanism and regulation of class switch recombination. *Annu. Rev. Immunol.* 26:261–292.
8. Corneo, B., R.L. Wendland, L. Deriano, X. Cui, I.A. Klein, S.Y. Wong, S. Arnal, A.J. Holub, G.R. Weller, B.A. Pancake, et al. 2007. Rag mutations reveal robust alternative end joining. *Nature.* 449:483–486.
9. Nussenzweig, A., and M.C. Nussenzweig. 2007. A backup DNA repair pathway moves to the forefront. *Cell.* 131:223–225.
10. Kotnis, A., L. Du, C. Liu, S.W. Popov, and Q. Pan-Hammarstrom. 2008. Nonhomologous emd-joining in class switch recombination: the beginning of the end. *Philos. Trans. R. Soc. Lond. B. Biol. Sci.* In press.
11. Pan-Hammarstrom, Q., A.M. Jones, A. Lahdesmaki, W. Zhou, R.A. Gatti, L. Hammarstrom, A.R. Gennery, and M.R. Ehrenstein. 2005. Impact of DNA ligase IV on nonhomologous end joining pathways

during class switch recombination in human cells. *J. Exp. Med.* 201:189–194.
12. Yan, C.T., C. Boboila, E.K. Souza, S. Franco, T.R. Hickernell, M. Murphy, S. Gumaste, M. Geyer, A.A. Zarrin, J.P. Manis, et al. 2007. IgH class switching and translocations use a robust non-classical end-joining pathway. *Nature.* 449:478–482.
13. Casellas, R., A. Nussenzweig, R. Wuerffel, R. Pelanda, A. Reichlin, H. Suh, X.F. Qin, E. Besmer, A. Kenter, K. Rajewsky, and M.C. Nussenzweig. 1998. Ku80 is required for immunoglobulin isotype switching. *EMBO J.* 17:2404–2411.
14. Manis, J.P., Y. Gu, R. Lansford, E. Sonoda, R. Ferrini, L. Davidson, K. Rajewsky, and F.W. Alt. 1998. Ku70 is required for late B cell development and immunoglobulin heavy chain class switching. *J. Exp. Med.* 187:2081–2089.
15. Rolink, A., F. Melchers, and J. Andersson. 1996. The SCID but not the RAG-2 gene product is required for Sm-Se heavy chain class switching. *Immunity.* 5:319–330.
16. Rooney, S., F.W. Alt, D. Lombard, S. Whitlow, M. Eckersdorff, J. Fleming, S. Fugmann, D.O. Ferguson, D.G. Schatz, and J. Sekiguchi. 2003. Defective DNA repair and increased genomic instability in Artemis-deficient murine cells. *J. Exp. Med.* 197:553–565.
17. Li, G., F.W. Alt, H.L. Cheng, J.W. Brush, P.H. Goff, M.M. Murphy, S. Franco, Y. Zhang, and S. Zha. 2008. Lymphocyte-specific compensation for XLF/cernunnos end-joining functions in V(D)J recombination. *Mol. Cell.* 31:631–640.
18. Rooney, S., F.W. Alt, J. Sekiguchi, and J.P. Manis. 2005. Artemis-independent functions of DNA-dependent protein kinase in Ig heavy chain class switch recombination and development. *Proc. Natl. Acad. Sci. USA.* 102:2471–2475.
19. Moshous, D., I. Callebaut, R. de Chasseval, B. Corneo, M. Cavazzana-Calvo, F. Le Deist, I. Tezcan, O. Sanal, Y. Bertrand, N. Philippe, et al. 2001. Artemis, a novel DNA double-strand break repair/V(D)J recombination protein, is mutated in human severe combined immune deficiency. *Cell.* 105:177–186.
20. Ege, M., Y. Ma, B. Manfras, K. Kalwak, H. Lu, M.R. Lieber, K. Schwarz, and U. Pannicke. 2005. Omenn syndrome due to ARTEMIS mutations. *Blood.* 105:4179–4186.
21. Moshous, D., C. Pannetier, R. Chasseval Rd, F. Deist Fl, M. Cavazzana-Calvo, S. Romana, E. Macintyre, D. Canioni, N. Brousse, A. Fischer, et al. 2003. Partial T and B lymphocyte immunodeficiency and predisposition to lymphoma in patients with hypomorphic mutations in Artemis. *J. Clin. Invest.* 111:381–387.
22. Evans, P.M., L. Woodbine, E. Riballo, A.R. Gennery, M. Hubank, and P.A. Jeggo. 2006. Radiation-induced delayed cell death in a hypomorphic Artemis cell line. *Hum. Mol. Genet.* 15:1303–1311.
23. Riballo, E., M. Kuhne, N. Rief, A. Doherty, G.C. Smith, M.J. Recio, C. Reis, K. Dahm, A. Fricke, A. Krempler, et al. 2004. A pathway of double-strand break rejoining dependent upon ATM, Artemis, and proteins locating to gamma-H2AX foci. *Mol. Cell.* 16:715–724.
24. Franco, S., M.M. Murphy, G. Li, T. Borjeson, C. Boboila, and F.W. Alt. 2008. DNA-PKcs and Artemis function in the end-joining phase of immunoglobulin heavy chain class switch recombination. *J. Exp. Med.* 205:557–564.
25. Peake, J., A. Waugh, F. Le Deist, A. Priestley, F. Rieux-Laucat, N. Foray, E. Capulas, B.K. Singleton, J.P. de Villartay, A. Cant, et al. 1999. Combined immunodeficiency associated with increased apoptosis of lymphocytes and radiosensitivity fibroblasts. *Cancer Res.* 59:3454–3460.
26. Pan, Q., C. Petit-Frere, A. Lahdesmaki, H. Gregorek, K.H. Chrzanowska, and L. Hammarstrom. 2002. Alternative end joining during switch recombination in patients with ataxia-telangiectasia. *Eur. J. Immunol.* 32:1300–1308.
27. Peron, S., Q. Pan-Hammarstrom, K. Imai, L. Du, N. Taubenheim, O. Sanal, L. Marodi, A. Bergelin-Besancon, M. Benkerrou, J.P. de Villartay, et al. 2007. A primary immunodeficiency characterized by defective immunoglobulin class switch recombination and impaired DNA repair. *J. Exp. Med.* 204:1207–1216.
28. Pan-Hammarstrom, Q., S. Dai, Y. Zhao, I.F. van Dijk-Hard, R.A. Gatti, A.L. Borresen-Dale, and L. Hammarstrom. 2003. ATM is not required in somatic hypermutation of VH, but is involved in the introduction of mutations in the switch mu region. *J. Immunol.* 170:3707–3716.
29. Pan, Q., H. Rabbani, F.C. Mills, E. Severinson, and L. Hammarstrom. 1997. Allotype-associated variation in the human gamma3 switch region as a basis for differences in IgG3 production. *J. Immunol.* 158:5849–5859.
30. Pan-Hammarstrom, Q., A. Lahdesmaki, Y. Zhao, L. Du, Z. Zhao, S. Wen, V.L. Ruiz-Perez, D.K. Dunn-Walters, J.A. Goodship, and L. Hammarstrom. 2006. Disparate roles of ATR and ATM in immunoglobulin class switch recombination and somatic hypermutation. *J. Exp. Med.* 203:99–110.
31. Mills, F.C., M.P. Mitchell, N. Harindranath, and E.E. Max. 1995. Human Ig S gamma regions and their participation in sequential switching to IgE. *J. Immunol.* 155:3021–3036.
32. Ma, Y., U. Pannicke, K. Schwarz, and M.R. Lieber. 2002. Hairpin opening and overhang processing by an Artemis/DNA-dependent protein kinase complex in nonhomologous end joining and V(D)J recombination. *Cell.* 108:781–794.
33. Schrader, C.E., J.E. Guikema, E.K. Linehan, E. Selsing, and J. Stavnezer. 2007. Activation-induced cytidine deaminase-dependent DNA breaks in class switch recombination occur during G1 phase of the cell cycle and depend upon mismatch repair. *J. Immunol.* 179:6064–6071.
34. Drouet, J., P. Frit, C. Delteil, J.P. de Villartay, B. Salles, and P. Calsou. 2006. Interplay between Ku, Artemis, and the DNA-dependent protein kinase catalytic subunit at DNA ends. *J. Biol. Chem.* 281:27784–27793.
35. Ma, Y., K. Schwarz, and M.R. Lieber. 2005. The Artemis:DNA-PKcs endonuclease cleaves DNA loops, flaps, and gaps. *DNA Repair (Amst.).* 4:845–851.
36. Niewolik, D., U. Pannicke, H. Lu, Y. Ma, L.C. Wang, P. Kulesza, E. Zandi, M.R. Lieber, and K. Schwarz. 2006. DNA-PKcs dependence of Artemis endonucleolytic activity, differences between hairpins and 5′ or 3′ overhangs. *J. Biol. Chem.* 281:33900–33909.
37. Tsai, C.J., S.A. Kim, and G. Chu. 2007. Cernunnos/XLF promotes the ligation of mismatched and noncohesive DNA ends. *Proc. Natl. Acad. Sci. USA.* 104:7851–7856.
38. Yannone, S.M., I.S. Khan, R.Z. Zhou, T. Zhou, K. Valerie, and L.F. Povirk. 2008. Coordinate 5′ and 3′ endonucleolytic trimming of terminally blocked blunt DNA double-strand break ends by Artemis nuclease and DNA-dependent protein kinase. *Nucleic Acids Res.* 36:3354–3365.
39. van der Burg, M., N.S. Verkaik, A.T. den Dekker, B.H. Barendregt, I. Pico-Knijnenburg, I. Tezcan, J.J. van Dongen, and D.C. van Gent. 2007. Defective Artemis nuclease is characterized by coding joints with microhomology in long palindromic-nucleotide stretches. *Eur. J. Immunol.* 37:3522–3528.
40. Pan, Q., C. Petit-Frere, S. Dai, P. Huang, H.C. Morton, P. Brandtzaeg, and L. Hammarstrom. 2001. Regulation of switching and production of IgA in human B cells in donors with duplicated alpha1 genes. *Eur. J. Immunol.* 31:3622–3630.
41. Pan, Q., H. Rabbani, and L. Hammarstrom. 1998. Characterization of human gamma 4 switch region polymorphisms suggests a meiotic recombinational hot spot within the Ig locus: influence of S region length on IgG4 production. *J. Immunol.* 161:3520–3526.
42. Noordzij, J.G., N.S. Verkaik, M. van der Burg, L.R. van Veelen, S. de Bruin-Versteeg, W. Wiegant, J.M. Vossen, C.M. Weemaes, R. de Groot, M.Z. Zdzienicka, et al. 2003. Radiosensitive SCID patients with Artemis gene mutations show a complete B-cell differentiation arrest at the pre-B-cell receptor checkpoint in bone marrow. *Blood.* 101:1446–1452.
43. van Zelm, M.C., C. Geertsema, N. Nieuwenhuis, D. de Ridder, M.E. Conley, C. Schiff, I. Tezcan, E. Bernatowska, N.G. Hartwig, E.A. Sanders, et al. 2008. Gross deletions involving IGHM, BTK, or Artemis: a model for genomic lesions mediated by transposable elements. *Am. J. Hum. Genet.* 82:320–332.